Electron-cyclotron-resonance heating in Wendelstein 7-X: A versatile heating and current-drive method and a tool for in-depth physics studies

To cite this article: R C Wolf *et al* 2019 *Plasma Phys. Control. Fusion* **61** 014037

OPEN ACCESS
IOP Publishing
Plasma Physics and Controlled Fusion
Plasma Phys. Control. Fusion **61** (2019) 014037 (9pp)
https://doi.org/10.1088/1361-6587/aaeab2

Electron-cyclotron-resonance heating in Wendelstein 7-X: A versatile heating and current-drive method and a tool for in-depth physics studies

R C Wolf[1], S Bozhenkov[1], A Dinklage[1], G Fuchert[1], Y O Kazakov[2], H P Laqua[1], S Marsen[1], N B Marushchenko[1], T Stange[1], M Zanini[1], I Abramovic[3], A Alonso[4], J Baldzuhn[1], M Beurskens[1], C D Beidler[1], H Braune[1], K J Brunner[1], N Chaudhary[1], H Damm[1], P Drewelow[1], G Gantenbein[5], Yu Gao[6], J Geiger[1], M Hirsch[1], U Höfel[1], M Jakubowski[1], J Jelonnek[5], T Jensen[8], W Kasparek[8], J Knauer[1], S B Korsholm[7], A Langenberg[1], C Lechte[7], F Leipold[7], H Trimino Mora[1], U Neuner[1], S K Nielsen[7], D Moseev[1], H Oosterbeek[1], N Pablant[9], E Pasch[1], B Plaum[8], T Sunn Pedersen[1], A Puig Sitjes[1], K Rahbarnia[1], J Rasmussen[7], M Salewski[7], J Schilling[1], E Scott[1], M Stejner[7], H Thomsen[1], M Thumm[5], Y Turkin[1], F Wilde[1] and the Wendelstein 7-X Team[10]

[1] Max-Planck-Institut für Plasmaphysik, Greifswald, Germany
[2] Laboratory for Plasma Physics, LPP-ERM/KMS, Brussels, Belgium
[3] Technical University of Eindhoven, Eindhoven, The Netherlands
[4] Laboratorio Nacional de Fusión, CIEMAT, Madrid, Spain
[5] Karlsruhe Institute of Technology, IHM, Karlsruhe, Germany
[6] Forschungszentrum Jülich, IEK-4, Jülich, Germany
[7] Technical University of Denmark, Kgs. Lyngby, Denmark
[8] IGVP, University of Stuttgart, Germany
[9] Princeton Plasma Physics Laboratory, Princeton, NJ, íUnited States of America

E-mail: robert.wolf@ipp.mpg.de

Received 6 July 2018, revised 19 September 2018
Accepted for publication 23 October 2018
Published 27 November 2018

Abstract

For stellarators, which need no or only small amounts of current drive, electron-cyclotron-resonance heating (ECRH) is a promising heating method even for the envisaged application in a fusion power plant. Wendelstein 7-X (W7-X) is equipped with a steady-state capable ECRH system, operating at 140 GHz, which corresponds to the 2nd cyclotron harmonic of the electrons at a magnetic field of 2.5 T. Ten gyrotrons are operational and already delivered 7 MW to W7-X plasmas. Combined with pellet injection, the highest triple product (0.68×10^{20} keV m^{-3} s), observed up to now in stellarators,

[10] See author list of R C Wolf *et al* 2017 *Nucl. Fusion* **57** 102020.

was achieved (Sunn Pedersen *et al* 2018 *Plasma Phys. Control. Fusion* **61** 014035). For the first time, W7-X plasmas were sustained by 2nd harmonic O-mode heating, approaching the collisionality regime for which W7-X was optimized. Power deposition scans did not show any indication of electron temperature profile resilience. In low-density, low-power plasmas a compensation of the bootstrap current with electron-cyclotron current drive (ECCD) was demonstrated. Sufficiently strong ECCD close to the plasma centre produced periodic internal plasma-crash events, which coincide with the appearance of low order rationals of the rotational transform.

Keywords: stellarator, Wendelstein 7-X, electron-cyclotron-resonance heating and current drive

(Some figures may appear in colour only in the online journal)

1. Introduction

The main objective of the optimized stellarator Wendelstein 7-X (W7-X) is to demonstrate that the underlying magnetic confinement concept fulfils the basic requirements for the development of fusion power plants [1, 2]. For this purpose, the design of W7-X is based on an elaborate optimization procedure which includes improved confinement of the thermal plasma and the fast ions, acceptable plasma equilibrium and stability properties up to $\langle\beta\rangle = 5\%$, and a magnetic field configuration, which is compatible with a resonant magnetic island divertor configuration for controlled heat and plasma exhaust [3, 4]. To this end, plasma currents were minimized aiming at reducing the β-effects on plasma equilibrium properties. This requires small Pfirsch–Schlüter currents, and hence a small Shafranov-shift, along with small bootstrap currents, which are an order of magnitude smaller than in equivalent tokamaks. The effect of the magnetic field configuration on the bootstrap current was investigated already in the first experimental campaign of W7-X [5]. Small bootstrap currents are a prerequisite for the magnetic island divertor which utilizes a magnetic field configuration with a rotational transform $\iota = 1$ at the plasma edge. Together with low magnetic shear, this resonance condition produces large magnetic islands which, when intersected by target plates, act as a divertor configuration for controlled heat and particle exhaust. Because of the resonance condition, the whole divertor configuration including strike line positions is very sensitive to net toroidal plasma currents. Towards the plasma centre the ι-profile drops slightly below one, avoiding major resonances in the confinement region of the plasma, which is a necessary condition for good confinement.

Commissioning and plasma operation of Wendelstein 7-X is following a staged approach [6, 7]. The three major steps are: (1) the commissioning of the basic device, including first cool-down of the cryostat and operation of the 70 superconducting coils, and first plasma operation took place in 2015/2016. The plasmas in the first experimental campaign (OP1.1) were bounded by five inboard limiters restricting the plasma pulses to 4 MJ integrated heating power. Major results of OP1.1 are summarized in [8–10]. (2) In a next step, W7-X was equipped with an uncooled divertor extending the pulse energy to 80 MJ. Experiments started in 2017 (campaign OP1.2a) and will continue in 2018 (OP1.2b). (3) Finally, full active cooling will be implemented by 2020/2021. Major components of this upgrade are a divertor cryo-pump and a steady-state divertor, designed and built for heat fluxes up to 10 MW m^{-2}. At 10 MW of heating power, the envisaged pulse duration is 30 min, corresponding to 18 GJ of pulse energy. While the overall active cooling capability of W7-X is designed to dissipate 10 MW over 30 min, the details of the plasma scenario for which this can be achieved is still a matter of investigation and will also have to be studied experimentally. Considerations for finding suitable plasma scenarios include the influence of the magnetic configuration on local heat fluxes reaching plasma-facing components, the level of stray-radiation, caused by non-absorbed electron-cyclotron-resonance heating (ECRH) power, which can be dissipated by in-vessel structures, and the capability to monitor and control in-vessel components guaranteeing safe operation within their design margins.

The resonant coupling of microwaves to the gyro-motion of the electrons in the plasma is a very versatile heating method. Depending on the launch angle, both, heating and current-drive can be realized [11]. In stellarators, ECRH has the potential to become the heating method even for a device on the scale of a power plant. There are three reasons for this. Firstly, stellarators need little or no external current drive to produce and maintain a steady-state plasma. Therefore, the lower current-drive efficiency of ECRH compared to other current drive methods, such as neutral beam injection or lower hybrid current drive, should not be an issue. Secondly, achieving high fusion power requires high plasma densities. Assuming $\langle\sigma v\rangle_{DT} \sim T^2$ (where n and T are the ion density and temperature, and $\langle\sigma v\rangle_{DT}$ the Maxwell averaged DT-fusion cross-section), the fusion power scales as $n^2T^2 \sim \beta^2B^4$ (B being the magnetic field strength). Stellarators have an additional perspective to this. Neoclassical transport in stellarators in the $1/\nu$-collisionality regime scales as $\varepsilon_{eff}{}^{3/2}\, T^{7/2}/(n\, B^2\, R^2)$, where ε_{eff} is the effective helical ripple, T and n are the plasma temperature and density, B is the magnetic field and R the major radius of the toroidal device [12]. Stellarator optimization, aiming at a reduction of this intrinsic transport level, attempts to minimize ε_{eff}, which depends on the magnetic field configuration. Nevertheless, the dependence on $T^{7/2}/n$ strongly favours moderate temperatures and high densities, as long as the temperature is high enough for achieving fusion conditions. At densities above 10^{20} m^{-3} the collisional coupling of the electrons and ions is strong enough to generate high ion temperatures with a heating method such as ECRH, which couples its power to the electrons. For W7-X, realizing the $1/\nu$-regime means that the polarization of the ECRH has to be changed from the 2nd harmonic X-mode (X2) to 2nd harmonic O-mode (O2). At a resonant microwave

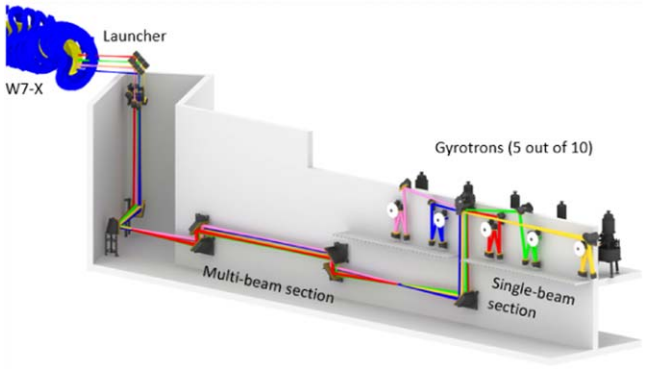

Figure 1. Illustration of one-half of the W7-X ECRH facility (reproduced with permission from [22]). The gyrotron beams are collected in the single-beam section and optically transmitted together over approximately 30 m in the multi-beam section, before they are divided into single beams again near the launchers. The other half of the facility (not shown) is a mirror image of the one shown.

frequency of 140 GHz, the X2 cut-off density lies at $1.2 \times 10^{20}\,\mathrm{m}^{-3}$. Plasma breakdown and plasma heating below this density require X2-heating. Above this density, up to $1.8 \times 10^{20}\,\mathrm{m}^{-3}$ O2-heating has to be applied. The actual O2 cut-off lies at $2.4 \times 10^{20}\,\mathrm{m}^{-3}$, however, is practically not attainable by O2-ECRH. Thirdly, ECRH waves entering the plasma vessel have a very high power density (approximately $200\,\mathrm{MW\,m}^{-2}$ in the case of remote steering launchers [13]) making large openings or antennas for coupling the power into the plasma obsolete. In addition, microwaves can be transmitted over distances of several tens of meters without excessive losses using quasi-optical transmission through air or waveguides so that the gyrotrons, generating the microwaves, can be positioned far away from the plasma device.

In addition, ECRH is characterized by a local heat deposition. For the magnetic field gradients of W7-X in the proximity of the magnetic axis of about $0.5\,\mathrm{T\,m}^{-1}$, the radial width of the X2-power deposition profile, as given by the resonance condition, is between 3 and 5 mm (depending on plasma parameters). The vertical width, given by the diameter of the microwave beam, is about 12 cm. Both dimensions are small compared to the average minor radius of the plasma of 55 cm. By moving the ECRH beam vertically or by changing the magnetic field and thus moving the resonance layer radially, the position of the power deposition inside the plasma can be controlled. As a result, ECRH is an ideal tool for studying the effect of the power deposition on plasma transport. Using power-modulated ECRH [11], the propagation of heat waves reveals the non-linear relation between the heat flux and temperature gradient [14]. Launching microwaves in the toroidal direction produces a radially localized electrical current, opening up the possibility for current control schemes. In W7-X, even small toroidal currents have a profound effect on the rotational transform [15] changing the resonance condition of the magnetic island divertor at the plasma edge or inducing low order resonances in the plasma core affecting plasma transport and stability.

Finally, ECRH has direct or indirect implications for in-vessel components and diagnostic applications. In case of incomplete absorption of microwaves by the plasma, high ECRH powers lead to significant levels of stray-radiation. In particular, for long-pulse or steady-state operation all in-vessel components have to be specially designed, avoiding undue absorption of stray-radiation which could lead to an overheating of the component. W7-X is designed for a stray-radiation level of 1 MW [16, 17], assuming a maximum of 10% of non-absorbed heating power. Another issue concerns microwave diagnostics, which rely on measuring the plasma emission near the ECRH frequency such as electron-cyclotron emission (ECE). Here, very efficient notch filters are required to suppress the high stray-radiation power level at the heating frequency. A particular challenge is the realization of a collective Thomson scattering (CTS) measurement system using one of the heating gyrotrons for wave scattering. Besides the modulation of the gyrotron to discriminate between ECE and scattered radiation, a 120 dB notch filter is required to cut out the 140 GHz background from the scattering spectrum. A first such system was successfully demonstrated on ASDEX Upgrade [18]. On W7-X a similar version was installed and tested successfully during the last campaign [19].

This paper focuses on ECR heating and current drive experiments and related physics studies of the experimental campaign OP1.2a. A more general overview of the first W7-X results using a divertor configuration is presented in [20].

2. The Wendelstein 7-X electron-cyclotron-resonance heating system

ECRH is currently the only heating system available on W7-X [21, 22]. Neutral beam injection [23] and ion-cyclotron-resonance heating [24] are in preparation. The W7-X ECRH is based on gyrotrons with a frequency of 140 GHz corresponding to 2nd harmonic heating at 2.5 T or 3rd harmonic heating at 1.7 T. The high-power gyrotrons were designed and tested for cw-operation up to 30 min. The maximum output power levels range from 700 kW to 1 MW. All W7-X gyrotrons also operate at 104 GHz, however, at about half the power. Plasma heating at 104 GHz, however, would require modifications of the transmission line.

During OP1.1 six gyrotrons were in operation, delivering up to 4.3 MW to the plasma. For OP1.2a ten gyrotrons were available. The maximum heating power coupled to the plasma was just above 7 MW. The longest plasmas at reduced ECRH power lasted 30 s (#20171206.017). A unique feature of the ECRH at W7-X is the transmission of the microwaves from the gyrotrons to the torus using a quasi-optical mirror system in air. Each microwave beam travels over 18 mirrors to the launchers which form the interface between the transmission line (in air) and the plasma. Figure 1 illustrates the arrangement of the ECRH facility with respect to W7-X. The standard set-up uses four front-steering launchers (equipped with three launch positions each) which can steer the microwave beams in the vertical and toroidal direction. The overall transmission efficiency was experimentally estimated to be 94% [10, 22], which is close to the theoretical value. In addition, two beams can be relayed to two remote steering launchers. One of their purposes

is to test this new technology, which, because of the very high power density and the absence of any movable part near the plasma [13], is a prospective candidate for heating a power plant plasma. While the front steering launchers are located at the low field side of W7-X and at a toroidal position where the magnetic field has a maximum, the remote steering launchers are installed near the minimum of the magnetic field. Simulations indicate that this feature can be used to selectively heat trapped and passing electrons [25].

3. ECR heating scenarios and plasma transport

The ECRH scenarios, established up to now, are 2nd harmonic X-mode (X2) and 2nd harmonic O-mode (O2) at 140 GHz. Since ECRH transfers the power directly to the plasma electrons, ion heating depends on the collisional energy transfer from electrons to ions and thus on the plasma density. In contrast to tokamaks, a significant part of core confinement in stellarators is governed by neoclassical transport [26]. Since plasma transport in stellarators is not intrinsically ambipolar, the ambipolarity condition for the electron and ion fluxes $\Gamma_e(E_r) = \sum Z_i \Gamma_i(E_r)$ determines the radial electric field, E_r. Depending on the ratio between electron and ion temperatures, T_e/T_i, and on the plasma collisionality, different solutions or roots of the ambipolarity equation can develop. For the results reported here, at low plasma densities (line-averaged densities of about 2–3 $\times$ $10^{19}\,\mathrm{m}^{-3}$) and strong central electron heating, T_e is much larger than T_i. Correspondingly, the central parts of the plasma are in the $\sqrt{\nu}$-regime with $E_r > 0$ (electron root). The positive E_r, reducing the outward electron flux, governs the electron transport. Generally, in W7-X a few MW of ECRH are enough to produce central electron temperatures between 5 and 10 keV [5, 8–10]. The ions remain relatively cold with $T_i < 2$ keV. Increasing the density and thus the collisionality, electron transport is governed by the $1/\nu$-regime which is characterized by a transport coefficient $D_{1/\nu} \sim \varepsilon_{eff}^{3/2}\, T^{7/2}/n$. Stellarator optimization aims at minimizing ε_{eff} to compensate the unfavourable temperature scaling of the $1/\nu$-transport. Depending on the magnetic field configuration, W7-X ε_{eff} typically remains near 1% over most of the plasma cross-section. The highest performance plasmas achieved during OP1.2a were already were in the $1/\nu$-regime for the electrons with the ion-root solution for the electric field. Transiently (over a period of approximately 200 ms), the highest triple product achieved was $n_i\ T_i\ \tau_E = 0.68 \times 10^{20}\,\mathrm{keV\,m^{-3}\,s}$ (#20171207.006). The underlying plasma parameters are $T_{i0} = T_{e0} = 3.8$ keV, $n_{e0} = 0.9 \times 10^{20}\,\mathrm{m}^{-3}$ and $\tau_E = 220$ msec. For the calculation of the ion density, a Z_{eff} of 1.5 was assumed (assuming carbon as the main impurity species). The ECRH power applied was 5 MW. While this example is mentioned here, as it demonstrates what could be achieved with X2-heating, more details about this high performance plasma are reported in [20].

The confinement times of many of the W7-X plasmas of the first experimental campaign (OP1.1) agree well with the ISS04 confinement scaling [27, 28]. This trend could be confirmed in the divertor configuration of OP1.2a. In fact, the confinement time of the high performance plasma mentioned above lies above the scaling (by about 50% and only for about one confinement time). It is currently investigated if the improved confinement phase can be sustained over several energy confinement times and, hence, if the observed regime is suitable for steady-state operation. Studies of the link between ECRH power and achievable density indicate the existence of a radiative density limit with a Sudo-like power scaling [29, 30]. Accordingly, limited heating power and relatively high impurity fractions prevented high density operation in OP1.1 limiter plasmas. Although hydrogen fuelling compared to helium fuelling appeared to be less efficient in OP1.2a divertor plasmas, high densities in hydrogen and mixed hydrogen/helium plasmas could be achieved using hydrogen pellet injection [20]. However, the technical capabilities of the pellet injector limited the period of the pellet injection to about 2 s at an injection frequency of 30 Hz. Maximum line-integrated densities achieved were $1.4 \times 10^{20}\,\mathrm{m}^{-2}$ (#20171115.039). The maximum central density was $1.5 \times 10^{20}\,\mathrm{m}^{-3}$, lying well above the X2 cut-off density of $1.2 \times 10^{20}\,\mathrm{m}^{-3}$.

4. Plasma heating approach beyond the X2 cut-off

Advancing into the $1/\nu$-transport regime and, at the same time, minimizing the neoclassical transport by keeping the ratio of temperature to density small, requires 2nd harmonic O-mode heating above the X2 cut-off. This also guarantees that the ion temperature is similar to the electron temperature, despite using an electron heating method. In contrast to X2-heating, which has a single-pass absorption close to a 100%, the single-pass absorption of O2-heating is only around 70%, strongly depending on the electron temperature and the incidence angle of the ECRH-beam. In W7-X, 70% single-pass absorption should be achieved at $T_e = 3$ keV and $n_e = 10^{20}\,\mathrm{m}^{-3}$. The principle problem is that the absorption drops quadratically with decreasing temperature, potentially leading to a loss of ECRH power absorption as the density is raised.

To avoid such a scenario, a multi-pass absorption scheme is required [22]. Before OP1.2a, tiles made of molybdenum and covered with tungsten were mounted on the plasma-vessel wall opposite to the low-field-side launchers (in OP1.1 plane graphite tiles were used). Similar to the tiles used in ASDEX Upgrade [31], the surface of the tiles has the shape of a holographic grating to ensure that the beams travel through the plasma centre. After the reflected beams have travelled through the plasma again, polished stainless steel tiles reflect any remaining power. Overall, the scheme ensures that all microwave beams from all gyrotrons transiting the plasma three times travel through the plasma centre.

During the first campaign (OP1.1), a plasma was sustained purely with O2-heating [10]. After plasma breakdown applying X2-heating, O2-heating was added and eventually the gyrotrons in X2-mode were turned off. With a single-pass absorption of ~70%, the overall absorption (after three passes) was ~90%. However, due to the lack of heating power and a suitable core fuelling scheme, the density stayed below the X2 cut-off throughout the plasma pulse (the line-averaged density did not exceed $3 \times 10^{19}\,\mathrm{m}^{-3}$). Accordingly, the central electron temperature did not drop below 5 keV. The

measured level of non-absorbed power or stray-radiation stayed well within the design margins of the in-vessel components [32].

In OP1.2a the O2-heating experiment was repeated with much improved technical capabilities. Holographic tiles, which direct the microwave beams through the plasma centre, replaced the first reflector tiles. The polarization of the gyrotrons beams was changed during the course of the experiment using for each gyrotron a combination of grooved rotatable mirrors which introduce phase shifts of $\lambda/4$ (introducing ellipticity to the originally linearly polarized beam) and $\lambda/2$ (for the rotation of the beam) [33]. The required polarization is matched to the magnetic field vector at the plasma edge, which was calculated by an equilibrium code. Subsequently, the polarization vectors of each beam are propagated backwards to the vacuum window position in the ECRH launchers and matched to the polarizer settings in the quasi-optical transmission line. In addition, the optimum polarization was verified by small variations of the polarization during X2-plasma experiments, evaluating, both, the absorption of the waves by the plasma (using sniffer probes) and the transmission through the plasma (using electron-cyclotron-absorption probes and measurements of the surface temperature increase of the plasma facing wall opposite to the launch positions). Because of the remotely adjustable polarization, the gyrotrons required for plasma breakdown in X2-mode, later in the plasma pulse could be used for O2-heating. Overall, more gyrotrons were available, supporting higher electron temperatures at higher densities. Finally, the higher ECRH power together with the pellet injector facilitated core plasma densities in excess of the X2 cut-off density of $1.2 \times 10^{20}\,\mathrm{m}^{-3}$.

Figure 2 shows the evolution of parameters of a plasma reaching densities beyond the X2 cut-off in the plasma centre [34]. After plasma breakdown with three gyrotrons in X2-mode (using helium as a fuelling gas), two gyrotrons beams were turned off (still in X2-mode) and six gyrotrons in O2-mode were added (to understand the related power-steps, one has to know that the gyrotrons have different output-powers). The polarization of the remaining X2-gyrotron beams was changed from X2- to O2-mode, while delivering power to the plasma (indicated in figure 2 by the blue-shaded region). The polarization of the two X2-gyrotrons, which were turned off just after plasma breakdown, was changed to O2-mode before they were turned on again (power-step in figure 2 at 3s). After starting hydrogen pellet injection, the central density increases to $1.5 \times 10^{20}\,\mathrm{m}^{-3}$. In the high-density phase, 5.6 MW (from nine gyrotrons) sustained and heated the plasma. The fact that the signals of an ECE channel close to 140 GHz drops to zero provides clear evidence for reaching the ECRH cut-off density (in figure 2 indicated by the area shaded in grey). The central electron temperature measured by Thomson scattering remained at 2.2 keV. The stray radiation signal (of a sniffer probe close to the ECRH launch positions in module 2) increased to $23\,\mathrm{kW\,m}^{-2}$. For comparison, the design value for in-vessel components is $50\,\mathrm{kW\,m}^{-2}$. The phase after the pellet injection stopped and the density started to drop again shows how sensitive the overall microwave

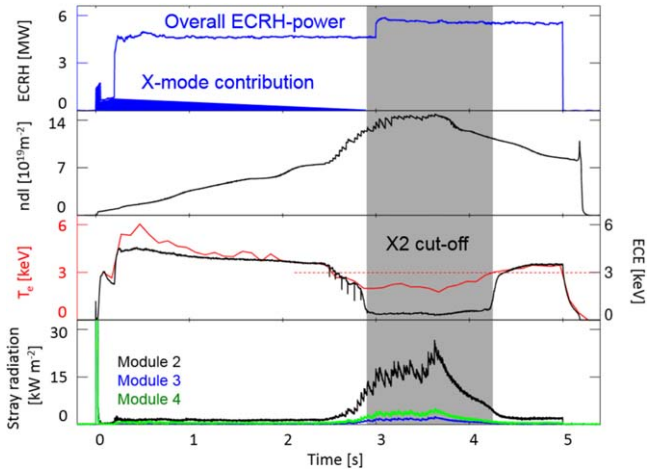

Figure 2. Evolution of the parameters of a plasma (#20171115.039) accomplishing O2-ECRH beyond the X2 cut-off. The top trace shows the total ECRH power and the X2-mode fraction. At 2.5 s pellet injection starts raising the line-integrated density from 0.7 to about $1.4 \times 10^{20}\,\mathrm{m}^{-2}$ (the laser path of the interferometer through the plasma is 1.3 m). The comparison of the central electron temperatures, as measured by Thomson scattering and ECE (close to 140 GHz), shows when the cut-off density is reached (shaded areas). The sniffer probe signals in the bottom trace indicates the stray radiation level at different positions (modules) inside the W7-X plasma vessel.

absorption reacts on the electron temperature. Although the central part of the plasma is still above the cut-off density, the increase of T_e from 2.2 keV to 2.9 keV decreases the stray-radiation level by more than a factor of two. The corresponding multi-pass absorption [34] increases from 70%–80% to 90% as derived from three sniffer probes which are treated in a model of coupled resonators. This example clearly shows that O2-heating is possible in W7-X. O2-heating was also achieved without pellet injection in helium plasmas with helium gas puffs (#20171114.036) just before a radiation collapse appeared. However, for sustaining the heating phase above the X2 cut-off over longer periods of time, a long-pulse or steady-state pellet injection system seems necessary.

5. Power deposition effects

As already found in other stellarator or heliotron experiments, in W7-X plasmas the location of the ECRH power deposition has a profound effect on the shape of the electron temperature profiles (see e.g. [35]). Comparing power balance and heat pulse transport coefficients, it seems that in many of the helical confinement devices the electron profile resilience in core confinement regions is less pronounced than in tokamaks or cannot be observed at all [36–39]. Comparison between the different experiments, however, is very difficult as the dominant transport mechanisms strongly depend on details of the experiment conditions (magnetic field configuration, collisionality, radial electric field, etc). This is the case, both, for anomalous [40, 41] and neoclassical transport. As pointed out

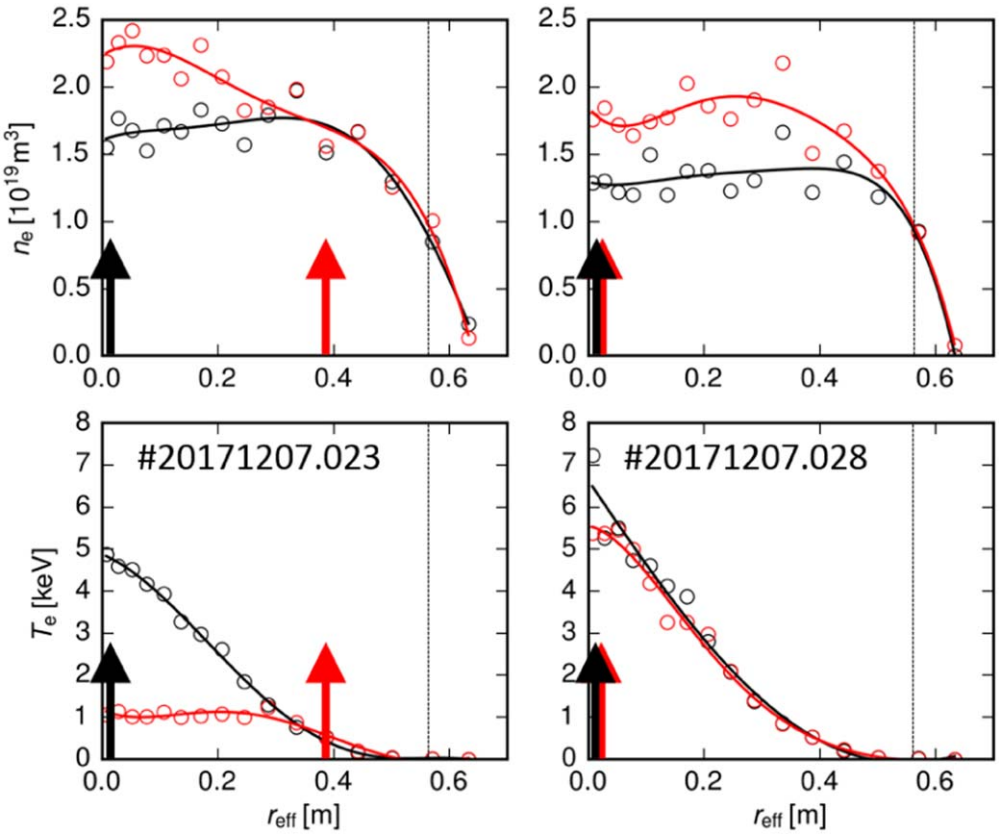

Figure 3. Electron density and temperature profiles (from Thomson scattering measurements) in plasmas with on- and off-axis X2 ECRH (as indicated by the black and red arrows). In #20171207.023, off-axis microwave beams replaced on-axis beams, in #20171207.028, also the second set of beams were heating the plasma centre. The Thomson scattering data shown are the average of two profiles (which are 100 ms apart, the solid lines are spline fits to the data points). The profiles of #20171207.023 were recorded at 0.4 s (on-axis) and 1.7 s (off-axis), the profiles of #20171207.028 at 0.3 s (on-axis) and 1.7 s (on-axis).

in the introduction, the latter plays a particular role in stellarators.

Already in OP1.1 limiter experiments, power deposition scans showed a strong effect on the electron temperature profiles [10, 42]. Moving the ECRH deposition from the centre of the plasma to a normalized radius of $r/a \approx 0.4$ completely flattened the electron temperature between plasma centre and deposition radius. In contrast, the density profiles showed a tendency to slightly peak towards the centre. Figure 3 shows a corresponding power deposition scan for OP1.2a divertor plasmas. Both plasmas were started with 2.5 MW on-axis heating power. In one case (#20171207.023), the on-axis microwave beams were replaced by off-axis beams (at a comparable power level) at $r_{eff} = 0.36$ m, corresponding to a normalized radius of $r/a \approx 0.7$. In the second case (#20171207.028), on-axis beams replaced the beams used for plasma breakdown. Apart from that, the plasmas were similar. Only off-axis heating (at a comparatively large radius) resulted in lower absorption of the ECRH, indicated by a higher stray radiation level. Eventually, this would have led to a radiation collapse, had the off-axis heating been continued. From the electron temperature profiles in figure 3 it is evident that peaked temperatures require central ECRH, not showing any indication of profile resilience inside the deposition radius. Compared to the OP1.1 results [10, 42], the power was increased from 0.6 MW to 2.5 MW and the deposition radius was moved further outwards, from $r/a \approx 0.4$ to 0.7.

Looking only at the plasma in which the ECRH deposition was moved to an off-axis position, one could conclude that the density profile peaks because of the change of the deposition radius. However, the plasma in which the power deposition remained in the centre also shows a density increase. A possible cause could be increased recycling due to the heating, in particular, of the divertor tiles (which are not water-cooled). Apart from the initial plasma phase, gas fuelling was not applied and hence did not contribute to the later density evolution.

The ECRH power deposition also changes with β. This has two reasons. First, the small but finite Shafranov-shift moves the magnetic axis away from the resonance position. Second, the diamagnetic effect reduces the magnetic field in the core, shifting both ECRH deposition and ECE measurement positions. Figure 4 illustrates these effects for the plasma which achieved the record triple product (#20171207.006, X2-heated plasma). At the beginning, when the central β-value is low ($\beta_0 \approx 0.4\%$), the ECRH deposition is in the plasma centre, as indicated by the power deposition profile calculated by the TRAVIS code [43]. During the plasma evolution β_0 increases to ≈3.7%. As the magnetic field drops and the axis shifts away from the ECRH resonance at 2.5 T, the deposition moves to

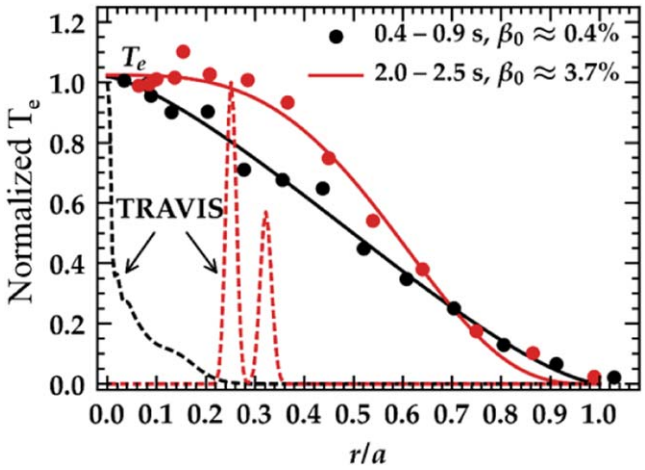

Figure 4. Shown are the normalized electron temperature profiles (from Thomson scattering measurements) for a plasma (#20171207.006) in which the central β increased from 0.4% (black) to 3.7% (red). The TRAVIS calculations (dashed curves) illustrate how the diamagnetic effect and the Shafranov-shift affect the ECRH power deposition profiles.

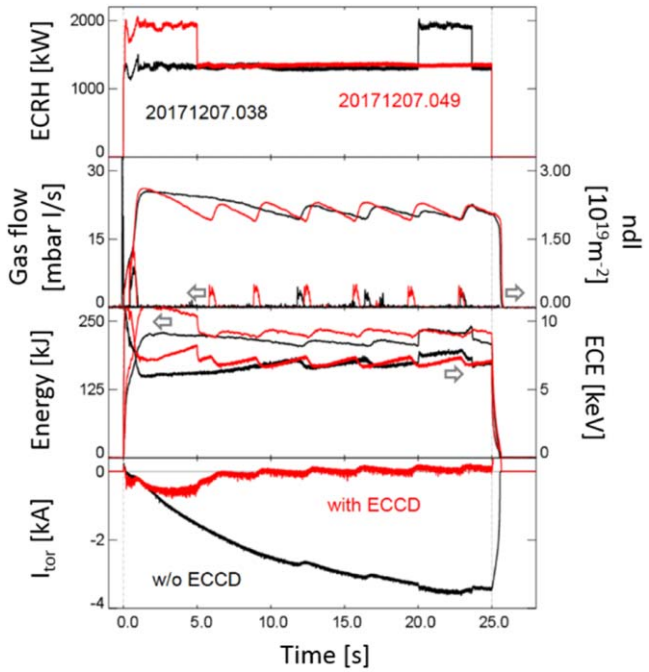

Figure 5. Comparison of two plasmas without (20171207.038) and with ECCD (20171207.049) to compensate the bootstrap current. The time traces (of ECRH power, gas flow and line integrated density, plasma energy, central electron temperature from ECE and plasma current) of the reference case without ECCD are plotted in black. In the counter-ECCD case (plotted in red), the total current (measured by a Rogowski coil) remains close to zero.

larger $r/a \approx 0.2$–0.3. Since the magnetic field gradient in W7-X is rather small, the resonance position reacts very sensitively to the diamagnetic effect. The comparison of the electron temperature profiles (normalized to the temperatures at the magnetic axis) shows that this influences the temperature profile shape in a similar way as is the case with deliberately shifting the deposition to larger radii. This example shows that the flattening of the electron temperature profiles inside the deposition radius can be observed also for ECRH powers above 5 MW and plasma densities up to $0.9 \times 10^{20}\,\mathrm{m}^{-3}$.

6. Electron-cyclotron current drive experiments

Electron-cyclotron current drive (ECCD) is a well-established method to produce toroidal currents non-inductively (see e.g. [44–46]). In a stellarator, such as W7-X, with low magnetic shear and small toroidal plasma currents, even small amounts of current drive have a profound effect on the ι-profile. In particular, the magnetic island divertor configuration of W7-X relies on maintaining the resonance condition, $\iota = 1$, at the plasma edge. However, the lowest neoclassical energy losses are expected in the so-called standard magnetic field configuration, which has a low but still significant bootstrap current contribution. To handle the influence of the bootstrap current evolution on the island divertor strike zones, several techniques were proposed [47]. One example is the scraper element. For OP1.2b a test version has been installed [48] which will be used to validate the passive protection of the edges of the divertor tiles. An alternative could be the application of ECCD to compensate the effect of the bootstrap current. In principle, this can be achieved in two different ways.

The first is to drive EC current opposite to the bootstrap current. This is illustrated in figure 5 for low density (divertor) plasmas in the standard magnetic field configuration. In the reference case without current drive, two gyrotrons with a total heating power of 1.5 MW were used to initiate and sustain the plasma. The density was controlled by the feedback of the gas injection using the dispersion interferometer for measuring the line integrated density. The slow oscillations seen on the plasma parameters (such as density, plasma energy and electron temperature) were caused by the controller which was not optimally adjusted at the time of the experiment. The main observation is a net toroidal current which is rising from zero to about −4 kA at 25 s. The rise time is determined by the L/R-time of the plasma which, depending on the electron temperature, is on the order of ∼30 s. In the example shown here, the toroidal current has almost fully developed after 25 s. The absolute value of the bootstrap current depends on the magnetic field configuration [47] and plasma pressure and thus on heating power and confinement. For plasmas with 5 MW of ECRH under certain conditions bootstrap currents of up to 50 kA are expected [47]. In the plasma with ECCD the launch angle of two gyrotron beams was changed from $\phi = 0$ to 1.5° (in toroidal direction) essentially keeping the total current at zero level, while all other plasma core parameters were similar. In the ECCD case, a third gyrotron at $\phi = 0$ was used for plasma breakdown. The example clearly shows that the compensation of the bootstrap current is possible, at least at low densities, where the current drive efficiency is high enough. At a line averaged density of $1.5 \times 10^{19}\,\mathrm{m}^{-3}$, as is the case in the example shown here, the current drive efficiency lies above $10\,\mathrm{kA\,MW}^{-1}$ (for $\phi = 10°$, $n_e = 5 \times 10^{19}\,\mathrm{m}^{-3}$ and 5 keV electron temperature, the current drive efficiency is

10 kA MW^{-1}). In a first analysis of the infra-red images of the divertor, the desired effect of compensation the bootstrap current can be observed. While without ECCD, depending on the toroidal plasma current, the strike lines move by a few centimetre [49], with ECCD essentially no movement can be seen.

Another possibility is the application of ECCD only during the initial phase of the plasma. The EC current, now in the direction of the bootstrap current, is dynamically adjusted in such a way that it anticipates the effect of the developing bootstrap current. The EC current has to be ramped down to the extent the plasma current (without ECCD) would build up [47]. Applying this scheme, it should be possible to avoid current drive at high plasma densities (beyond the X2-cutoff) where the ECCD efficiency is not sufficient to compensate the bootstrap current produced by the corresponding ECRH power. In addition, the necessity to continuously drive current would be avoided.

However, due to the low magnetic shear of W7-X, ECCD generally has the drawback that, if the current is driven close to the plasma centre, the ι-profile can form major resonances, as the ECCD induced ι-change scales like $\Delta\iota \sim I_{ECCD}/r^2$ (where I_{ECCD} is the driven current). Surprisingly, these resonances not only degrade the confinement but also lead to repetitive crashes of the electron temperature similar to sawtooth oscillations in tokamaks [10]. This indicates that the ι-resonances trigger some kind of pressure and/or current driven instability and that, as a result, a major redistribution of the plasma pressure inside the resonance radius takes place. Possible countermeasures could be a more even distribution of the ECCD current over the plasma cross-section. In this way, the local change of the rotational transform would be reduced and in the ideal case major resonances would be avoided [15, 47].

7. Summary and conclusions

To date, the ECRH facility at W7-X has coupled up to 7 MW into the plasma. As the only heating system, available initially, the reliable operation of the ECRH was a prerequisite for the success of the first two W7-X campaigns. ECRH was instrumental for achieving the highest triple product observed in a stellarator. Measures to increase the (time-averaged) heating power include a fast recovery of the gyrotron operation (within less than 1 ms) in case of a mode loss where in the past the gyrotron had to be shut down immediately [50].

Many important questions could already be addressed. O2-heating, which is necessary for achieving the W7-X objectives, was demonstrated for the first time. The results indicate that a prolongation of the O2 phase requires slightly lower densities or more heating power and a long-pulse pellet injector. Making use of the local heat deposition ($\leqslant$5 mm in radial and $\approx$12 cm in vertical direction), active power deposition scans (at ECRH powers up to 2.5 MW) do not give any indication of electron temperature profile resilience. For the development of high-β plasmas, with small but finite Shafranov-shift and a diamagnetic reduction of the magnetic field, this means that the plasma has to be initiated at a magnetic field above 2.5 T to maximize the central temperatures. For magnetic field configurations with a significant bootstrap current, ECCD could be one solution to compensate the effects of the bootstrap current on the magnetic island divertor. At least for low plasma densities, the full compensation of the bootstrap current by ECCD in the opposite direction was achieved. The feasibility of the more attractive scheme, which aims at anticipating the bootstrap current in the early phase of the plasma by exchanging the EC current against the developing toroidal current, depends on whether the formation of low order rational values of the rotational transform can be avoided.

Acknowledgments

This work has been carried out within the framework of the EUROfusion Consortium and has received funding from the EURATOM research and training programme 2014–2018 under grant agreement No 633053. The views and opinions expressed herein do not necessarily reflect those of the European Commission.

ORCID iDs

R C Wolf https://orcid.org/0000-0002-2606-5289
S Bozhenkov https://orcid.org/0000-0003-4289-3532

References

[1] Igitkhanov Y *et al* 2006 *Fusion Eng. Design* **81** 2695
[2] Wolf R C *et al* 2008 *Fusion Eng. Design* **83** 990
[3] Grieger G *et al* 1992 *Phys Fluids* B **4** 2081
[4] Renner H *et al* 2002 *Plasma Phys. Control. Fusion* **44** 1005
[5] Dinklage A *et al* 2018 *Nat. Phys.* **14** 855
[6] Wolf R C *et al* 2016 *IEEE Trans. Plasma Sience* **44** 1466
[7] Bosch H-S *et al* 2018 *IEEE Trans. Plasma Sience* **46** 1131
[8] Klinger T *et al* 2017 *Plasma Phys. Control. Fusion* **59** 014018
[9] Sunn Pedersen T *et al* 2017 *Phys. Plasmas* **24** 055503
[10] Wolf R C *et al* 2017 *Nucl. Fusion* **57** 102020
[11] Erckmann V and Gasparino U 1994 *Plasma Phys. Control. Fusion* **36** 1869
[12] Beidler C D *et al* 2011 *Nucl. Fusion* **51** 076001
[13] Lechte C *et al* 2017 *EPJ Web of Conferences* **147** 04004
[14] Lopes Cardozo N J 1995 *Plasma Phys. Control. Fusion* **37** 799
[15] Geiger J *et al* 2013 *Plasma Phys. Control. Fusion* **55** 014006
[16] Hathiramani D *et al* 2013 *Fusion Eng. Design* **88** 1232
[17] Bosch H-S *et al* 2013 *Nucl. Fusion* **53** 126001
[18] Stejner M *et al* 2016 *41st Int. Conf. on Infrared, Millimeter, and Terahertz waves (IRMMW-THz)* (https://doi.org/10.1109/IRMMW-THz.2016.7758538)
[19] Moseev D *et al* 2018 Collective thomson scattering diagnostic at Wendelstein 7-X *Rev. Sci. Instrum.*
[20] Sunn Pedersen T *et al* 2018 First results from divertor operation in Wendelstein 7-X *Plasma Phys. Control. Fusion* **61** 014035
[21] Erckmann V *et al* 2014 *AIP Conf. Proc.* **1580** 542
[22] Stange T *et al* 2017 *EPJ Web of Conferences* **157** 02008
[23] McNeely P *et al* 2013 *Fusion Eng. Design* **88** 1034

[24] Ongena J *et al* 2014 *Phys. Plasmas* **21** 061514
[25] Marushchenko N B *et al* 2015 *EPJ Web of Conferences* **87** 01007
[26] Helander P *et al* 2012 *Plasma Phys. Control. Fusion* **54** 124009
[27] Yamada H *et al* 2005 *Nucl. Fusion* **45** 1684
[28] Fuchert G *et al* 2018 *Nucl. Fusion* **58** 106029
[29] Sudo S *et al* 1990 *Nucl. Fusion* **30** 11
[30] Fuchert G *et al* 2017 *European Conf. on Circuit Theory and Design (ECCTD)* (https://doi.org/10.1109/ECCTD.2017.8093228)
[31] Wagner D *et al* 2016 *J Infrared Milli Terahz Waves* **37** 45–54
[32] Marsen S *et al* 2017 *Nucl. Fusion* **57** 086014
[33] Michel G *et al* 2013 *Fusion Eng. Design* **88** 903
[34] Stange T *et al* 2018 First demonstration of magnetically confined high temperature plasmas beyond the X2-cutoff density sustained by O2-heating only parameters *Phys. Rev. Lett.* submitted
[35] Weir G M *et al* 2015 *Phys. Plasmas* **22** 056107
[36] Eguilior S *et al* 2003 *Plasma Phys. Control. Fusion* **45** 105
[37] Inagaki S *et al* 2003 *Nucl. Fusion* **46** 133
[38] Ryter F *et al* 2006 *Plasma Phys. Control. Fusion* **48** B453
[39] Hirsch M *et al* 2008 *Plasma Phys. Control. Fusion* **50** 053001
[40] Xanthopoulos P *et al* 2014 *Phys. Rev. Lett.* **113** 155001
[41] Proll J H E *et al* 2016 *Plasma Phys. Control. Fusion* **58** 014006
[42] Hirsch M *et al* 2017 *Nucl. Fusion* **57** 086010
[43] Marushchenko N B *et al* 2014 *Comput. Phys. Commun.* **185** 165
[44] Coda S *et al* 2000 *Plasma Phys. Control. Fusion* **42** B311
[45] Nagasaki K *et al* 2008 *Plasma Fusion Res.* **3** S1008
[46] Bock A *et al* 2017 *Nucl. Fusion* **57** 126041
[47] Geiger J *et al* 2015 *Plasma Phys. Control. Fusion* **57** 014004
[48] Lumsdaine A *et al* 2015 *Fusion Eng. Design* **98–99** 1357
[49] Gao Y *et al* 2018 Effects of the tordoidal plasma currents on the strike-line movements of W7-X *45th EPS Conf. on Plasma Physics (Prague)*
[50] Braune H *et al* 2018 *EPJ Web of Conf./30th German-Russian Joint Meeting on ECRH and Gyrotrons (RGM2018)* (https://doi.org/10.1109/IRMMW-THz.2018.8510214)